

Research Article

Temperature-Aware Routing for Telemedicine Applications in Embedded Biomedical Sensor Networks

Daisuke Takahashi,¹ Yang Xiao,¹ Fei Hu,² Jiming Chen,³ and Youxian Sun³

¹Department of Computer Science, The University of Alabama, Tuscaloosa, AL 35487, USA

²Computer Engineering Department, Rochester Institute of Technology, Rochester, NY 14623, USA

³State Key Laboratory of Industrial Control Technology, Institute of Industrial Process Control, Zhejiang University, Hangzhou 310027, China

Correspondence should be addressed to Yang Xiao, yangxiao@ieee.org

Received 13 April 2007; Revised 3 November 2007; Accepted 2 December 2007

Recommended by Hui Chen

Biomedical sensors, called *in vivo* sensors, are implanted in human bodies, and cause some harmful effects on surrounding body tissues. Particularly, temperature rise of the *in vivo* sensors is dangerous for surrounding tissues, and a high temperature may damage them from a long term monitoring. In this paper, we propose a thermal-aware routing algorithm, called least total-route-temperature (LTRT) protocol, in which nodes temperatures are converted into graph weights, and minimum temperature routes are obtained. Furthermore, we provide an extensive simulation evaluation for comparing several other related schemes. Simulation results show the advantages of the proposed scheme.

Copyright © 2008 Daisuke Takahashi et al. This is an open access article distributed under the Creative Commons Attribution License, which permits unrestricted use, distribution, and reproduction in any medium, provided the original work is properly cited.

1. INTRODUCTION

Telemedicine enables doctors to carry out remote diagnoses far from the patients. There are many researches on mobile telemedicine, for example, [1–23]. Telemedicine can be defined as an information technology that enables doctors to perform medical consultations or diagnoses away from patients. In other words, doctors can remotely examine patients by viewing and asking symptoms via monitors and sound devices, and gathering physiological data through the telecommunication, with which another end is set up at the patients sites.

One application of telemedicine using wearable wireless body area network architecture aims to implant biomedical sensors in human bodies. This kind of biomedical sensors is called *in vivo* sensors. Like basic wearable vital sensors, the *in vivo* sensors can sample a variety of biometric data, and transmit them to practitioners terminals, such as PDAs or tablet PCs, using the shortrange wireless connectivity [1–5, 19]. Furthermore, communications between the *in vivo* sensors and the terminals often involve multihop transmissions to avoid entire energy consumption [1]. Currently, the *in vivo* sensors are applied to an artificial retina, glucose level monitoring, organ monitoring, and cancer detecting [2].

However, implanting biomedical sensors into human bodies may cause some harmful effects on surrounding body tissues. Since the *in vivo* sensors usually transmit or relay biomedical data to neighboring sensor nodes from time to time, heat caused by processing and communication will appear inside of human bodies. Obviously, this temperature rise of the *in vivo* sensors is dangerous for surrounding tissues, and a high temperature may damage them from a long-term monitoring [1, 3]. Thus, regarding the *in vivo* sensors, routing protocols need to be designed to suppress the temperature rise up to a predefined threshold, that is, data transmissions among the sensors should disperse around networks and not rely on only one route [1]. In addition, for the sake of reducing exposure of infrared radiation (IR) (a kind of electromagnetic radiation), consideration of power consumption of batteries is of importance. Because lower batteries require recharging by IR, easily expending battery life should be required to recharge often, and this increases exposing body tissues to IR and should be avoided [6–9]. Of course, the latency of the network communication is also considered for critical situations.

In this paper, we propose a least total-route-temperature (LTRT) protocol, in which nodes temperatures are converted into graph weights, and minimum temperature routes are

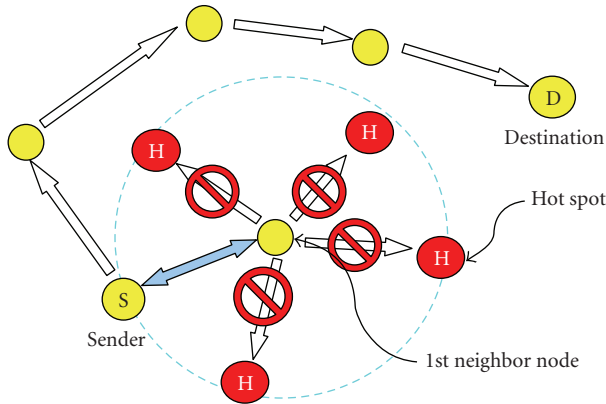


FIGURE 1: An example of TARA.

obtained. Furthermore, we provide an extensive simulation evaluation for comparing several other related schemes including the proposed scheme.

The rest of the paper is organized as follows. Section 2 provides a survey of thermal-aware routing algorithms. We propose the LTRT protocol in Section 3. Simulations are presented in Section 4. Finally, we conclude the paper in Section 5.

2. THERMAL-AWARE ROUTING ALGORITHMS

To avoid the heat generation, basically, three thermal-aware routing algorithms were proposed: thermal-aware routing algorithm (TARA), least temperature routing (LTR) protocol, and adaptive least temperature routing (ALTR) protocol [2]. In this section, we introduce these three thermal-aware routing algorithms.

2.1. Thermal-aware routing algorithm (TARA)

When biomedical sensors are implanted into human bodies, the temperature rise must be taken into account to avoid damaging surrounding body tissues. In addition, upon running out of batteries, the invivo sensors require to be recharged by IR radiation. However, this IR radiation also causes the temperature rise of the sensors. Therefore, the number of times to recharge sensor batteries is preferably reduced by prolonging battery life as long as possible [6–9].

Thermal-aware routing algorithm (TARA), shown in Figure 1, is designed for solving these constraints [6]. At first, TARA defines hot spots as areas where sensor nodes have relatively high temperature due to focusing data communications [6]. Upon detecting the hot spots, not to produce the temperature rise of these areas any longer, TARA attempts to establish another route to detour around the hot spots using a withdrawal strategy [6]. In this strategy, upon receiving packets, when surrounding (neighboring) nodes—except for a sending node—are all hot spots, current node will send back packets to the sender node, and the sender node will then select an alternative route to detour the hot spots or may send it back to its previous node, and so on [6]. After cooling a temperature of the hot spots down to a predefined limit,

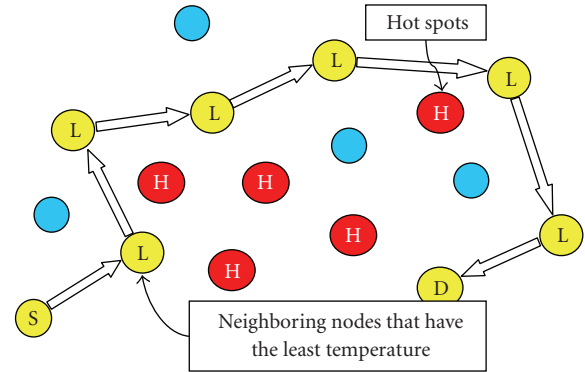


FIGURE 2: An example of LTR.

TARA takes these nodes into consideration as new candidates of later routing. To accomplish TARA effectively, every node must know temperature changes of neighboring nodes by always monitoring neighbors packet counts, and calculating communication radiation and power consumption to derive current temperature of the neighbors. The hot spots, which exceed a predefined minimum limit of temperature, must be checked by surrounding sensors, and later avoid participating in routing until temperature is standardized.

Figure 1 illustrates an example of TARA. A sender first tries to send packets to a neighboring node (1st neighboring node) that is on the way to the destination and not a hot spot. However, this neighboring node is surrounded by hot spots within its communication range. Therefore, it sends the packets back to the sender again, and the sender chooses an alternative node that is not a hot spot. The packets detour the hot spots to the destination as illustrated in Figure 1.

2.2. Least temperature routing (LTR)

Similar to TARA, least temperature routing (LTR) protocol, shown in Figure 2, is designed to avoid establishing routes on the hot spots aiming to keep temperature low in particular invivo sensor nodes [1]. However, unlike TARA, LTR always chooses neighboring nodes which have the lowest temperature for its routing [1]. Therefore, unless packets aim to be sent to a neighboring node which is the destination of the packets, current nodes always send the packets to the coolest neighbors and seek for the destination [1]. Besides, LTR also employs a packet discarding for the sake of maintaining the network bandwidth [1]. Each packet roaming in a network maintains its hop count by each hop. Compared with a predefined minimum hop count, namely, MAX_HOPS, if the value of the hop count exceeds MAX_HOPS, the current sensor node will throw away the packet from the network. In addition, to avoid infinitely looping the same route, packets wandering in a network can maintain a table which keeps track of sensor nodes that the packets have most recently passed through [1]. Thus, if a next node, where the packets will be forwarded (the coolest neighbor), is already on the table, the current node will pass the packets to the second lowest temperature node which is not on the table to avoid

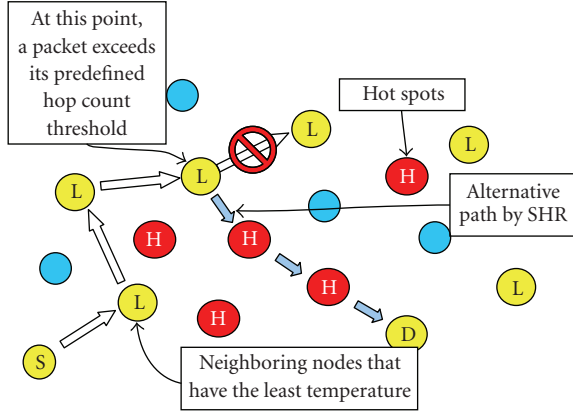


FIGURE 3: An example of ALTR.

choosing the same route. This consequently avoids infinitely looping over the same route. Figure 3 illustrates an example of LTR, which always chooses nodes that have the least temperature.

2.3. Adaptive least temperature routing (ALTR)

One variant of LTR protocol is adaptive least temperature routing (ALTR) protocol. A difference between LTR and ALTR is that while ALTR as in LTR employs a packet hop count and keeps track of the hop count of each packet in every hop, when the value of the hop count exceeds a predefined minimum hop count, namely, `MAX_HOPS_ADAPTIVE`, it can use the shortest hop-routing (SHR) protocol as an alternative protocol to take the packets to the destination as soon as possible [1]. From the name of “adaptive” least temperature routing, ALTR can adapt to particular topologies since in some network topologies, such as a ring topology, packet sequences inevitably trace the same path and temperature of sensor nodes on particular paths and the scheme will get higher rapidly, with a proactive delay mechanism utilized [1]. In this “proactive delay” mechanism, upon getting a packet from some neighboring node, when there are at most two ways to send the packet but their temperatures are comparatively high, the current node can wait a unit time for sending it to the coolest neighbor for the sake of calming down their temperature [1]. Although the packet latency somewhat becomes higher, the average temperature of networks can get lower [1]. Figure 3 illustrates an example of ALTR, which basically chooses nodes that have the least temperature until packets exceed a predefined hop-count threshold, `MAX_HOPS_ADAPTIVE`. Upon exceeding the threshold, packets simply choose nodes which can send them to the destination in the minimum hop count by using the shortest hop routing (SHR).

3. LEAST TOTAL-ROUTE TEMPERATURE (LTRT)

In this section, we first provide a discussion about thermal-aware routing algorithms. Then, we propose least total-route-temperature (LTRT) protocol.

In the previous section, we have briefly introduced three temperature-aware routing algorithms (e.g., TARA, LTR, and ALTR) to avoid the temperature rise of the invivo sensors inside human bodies due to sensor processing and communication. However, none of the three protocols accomplishes optimization for routings. For example, simulations in [1] show that compared with LTR and ALTR, TARA experiences the average delay as the packet arrival rate increases in both a 4×4 regular mesh network and a network of 50 densely connected nodes. This TARA’s average delay is basically caused by rerouting to alternative paths when packets encountered hot spots [1]. In addition, in both cases, TARA experiences both high power consumption of the entire network and high dropping packets [1]. Likewise, this high power consumption and high dropping packets come from a number of multihops to be required for packet forwarding [1].

In LTR, since sensor nodes keep passing packets to their neighboring nodes that have the least temperature unless one neighbor is the destination, in the worst case, most of the nodes will experience the packet passing, which wastes the precious network bandwidth, consumes extra battery power, and even raises temperature in the entire network. In short, since LTR does not initially schedule the route of packets but instead just chooses the least temperature nodes, the packets will basically detour to the destinations. In fact, LTR is a greedy approach, which may be locally optimal, but it is impossible to be globally optimal. Furthermore, in LTR, packets may go a wrong direction to the destination. Besides, since temperature of the sensor nodes will change every moment because even one data processing or communication will raise the sensor temperature, sequential packets will choose different routes, which may delay the entire data transmission. Moreover, in ALTR, although the hop count controls the routing strategy, it still wastes the network bandwidth as well as it may inevitably establish routes through the hot spots when utilizing SHR.

At last, in the context of lifetime of sensor networks (e.g., until 70% of all the nodes run out of power), in simulations in [1], TARA, LTR, and ALTR have shorter lifetime than SHR because, in nature, all three algorithms consume more power than SHR due to detouring.

Next, we propose a least total-route-temperature (LTRT) protocol.

As in LTR or ATRT, if algorithms always choose to send packets to the minimum-temperature neighboring nodes, the number of hops and the total temperature of the entire network will become large. This is because these algorithms are not designed to send packets toward destination nodes, but instead, they occasionally prefer to send packets to sensors having the minimum temperature but being located even in the opposite direction to destinations. This condition allows packets to stray in networks in a long period of time, resulting in unnecessary increase of hop counts and sensor temperature. Concerning these drawbacks from TARA, LTR, and ALTR, we propose another thermal aware-routing algorithm called least total route temperature (LTRT) protocol.

Our proposed LTRT protocol is designed to solve problems causing this redundant hops and total temperature rise. LTRT is designed to both choose routes that have the totally

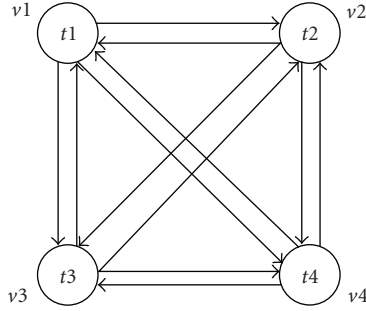


FIGURE 4: Node temperature.

least temperature from sender nodes to destination nodes and avoid wasting the network bandwidth by reducing the hop count. In other words, LTRT selects a least temperature route from all possible routes from a sender node to a destination, not always choosing the least temperature sensor nodes. In short, LTRT calculates routes from the single-source shortest path algorithms in graph theory (e.g., Dijkstra's algorithms) and applies these routes for later packet transmissions. With our expectation, LTRT will be positioned just between LTR and SHR and more efficient than ALTR. Therefore, like TARA, LTR, and ALTR, LTRT requires every node to assure temperature of its neighboring nodes from the received and transmitted packets.

To apply the single-source shortest path problem in graph theory to the thermal-aware routing problem, our protocol follows the next four steps.

- (1) Assign temperature of sensor nodes as weight to each sensor node from observation of communication activity by neighboring sensor nodes, shown in Figure 4.
- (2) In calculating routes, transfer weight (temperature) of sensor nodes to weight of edges ahead. For example, supposing that u and v are vertices (nodes) in directed graph G and (u, v) is an edge connecting vertices u and v (i.e., $u \rightarrow v$), then $w(u, v)$ (weight of (u, v)) is temperature of vertex u . This transfer is shown in Figure 5. Thus, upon transferring weight of each sensor node to the corresponding edges, temperature of destination nodes is just ignored.
- (3) By using the second graph, apply single-source shortest path algorithms to figure out routes having the least temperature from sending nodes to destination nodes.
- (4) To avoid excessively raising temperature of sensor nodes, periodically maintaining (updating) routes is required. The maintenance of routing also helps in adapting frequent network topology changes caused by node movements.

Figure 4 shows that from observing communication activity of neighboring nodes ($v1$, $v2$, $v3$, and $v4$), weight (temperature ($t1$, $t2$, $t3$, and $t4$)) of each sensor node can be calculated. At this point, temperature is just related to each sensor node.

Figure 5 shows that eight sensor nodes are transferred to corresponding directed edges ahead (e.g., $t1$ and $t2$). Now,

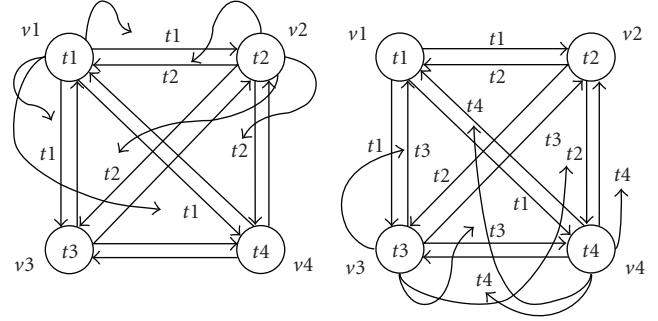


FIGURE 5: Building weight graph.

every edge is weighed according to weights of sensor nodes, and the edges come from constructing a weighted directed graph.

One tradeoff of the proposed scheme is that it requires sensor temperature to be transmitted among sensor nodes, and this operational overhead causes the battery consumption and temperature increase. Since the updating of sensor temperature is done periodically and the number of sensor nodes may not be large in the telemedicine application, the overhead can be tolerated and indicated in our simulations.

4. SIMULATIONS

To evaluate the temperature rise and the efficiency of power consumption of each algorithm, we wrote the simulation program by Java using discrete event simulation. Our simulations mainly consist of four events: route generation, sending packet, receiving packet, and periodically cooling down the temperature of every sensor node in the network. Instead of sending packets to a fixed base station, we rather choose the way in which the sender and the destination are selected randomly by each packet generation so that they can vary in every execution. We fixed the network topology as a mesh topology so that every sensor node in the network can be connected and send packets to any other node by using multihopping. In this topology setting, the number of sensor nodes can be changed so that we can measure the scalability of each algorithm in terms of the number of sensor nodes as well. The scalability is measured from 20 to 100 sensor nodes by a step of 10 sensor nodes.

Because of the simulation results from [1], at this time, comparisons are made among only three thermal-aware routing algorithms: the least total-route-temperature (LTRT, proposed) algorithm, the least temperature routing (LTR) algorithm, and the adaptive least temperature routing (ALTR) algorithm. Our simulations are based upon the transition of the increasing packet generation rate, where how many packets are generated in the unit time and the number of sensor nodes in the network, and three metrics are designed to evaluate the efficiency of each algorithm: average temperature rise, average hop count per arrival packet, where the metrics are interpreted into average delay of arrival packets, and percentage of lost packets.

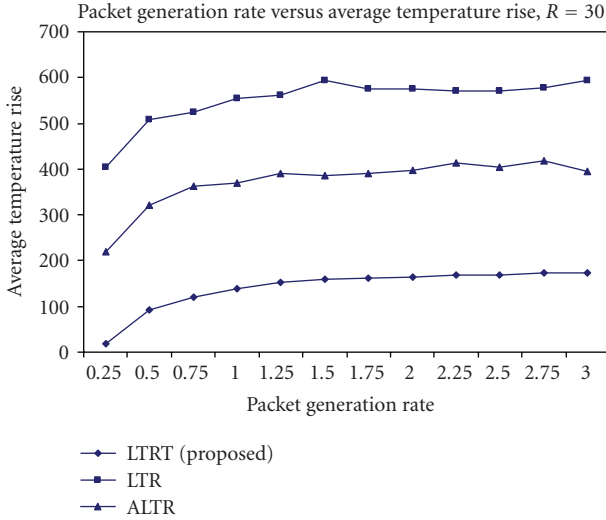


FIGURE 6: Packet generation rate versus average temperature rise with radio transmission range 30.

Each simulation continues iterating until totally 2000 packets are generated and either delivered to the destinations or discarded (recorded as lost packets), for example, the sum of the delivered packets and the lost packets reaches 2000. The sensor node temperature rises by 1 unit when they receive a packet, and initially every node has 1 unit of temperature. In these simulations, while we defined the minimum temperature of the sensor node as 1 unit, the maximum temperature was not defined or defined with infinity. Also, when time passes the specified period, which was set to 40 units of time in these simulations, the process reduces 1 unit of temperature from every sensor node. Since we assume that the power consumption will be in relation to the total hops performed in the network, in the simulations, we did not measure the power consumption separately.

Furthermore, by following the simulation setting in [1], we assume that the value of MAX_HOPS in LTR was equal to 40 and MAX_HOPS_ADAPTIVE in ALTR was 10 so that ALTR would change the routing algorithm from LTR to the shortest hop routing (SHR) algorithm at this threshold.

4.1. 5×10 mesh topology

In the 5×10 mesh topology simulation, we fix the number of sensor nodes equal to 50 while we increase the packet generation rate, where how many packets are generated per unit time, from 0.25 to 3.0.

4.1.1. Packet generation rate versus average temperature rise

When the radio transmission range is set to 30, since we set the distance of two adjacent nodes to 20, every sensor node has at least 3 neighboring nodes, where the nodes are at the corner, and some of sensor nodes can have 8 neighboring nodes. As shown in Figure 6, every of the three algorithms has the similar tendency, that is, in relation to the packet generation rate, the average temperature rise grows faster in the

range of 0.25 to 1 while after this range, they tend to become stable. However, since in LTR packets need to roam in the network until either they can reach the destination or exceed the predefined max hop count threshold, they keep the temperature of the entire network comparatively high resulting in the high average temperature. Instead, since our proposed LTRT determines a route to the destination before starting sending packets, it is impossible for packets to roam in the network and this affects the number of total hop counts required to reach the destination and consequently influences temperature rise of the entire network.

In case that the radio transmission range is 25, sensor nodes in the network have at least 2 neighbors up to 4 neighbors. In this case, the choice of the next sensor nodes for the routing is apparently reduced, and the average temperature rise gets higher than the case that the radio transmission range is 30. This is because, due to the reduction of the number of the neighbors, the probability that packets will arrive at the destination gets lower within certain hop counts than the case of the radio transmission range 30. Therefore, packets require extra travel around the network and consequently it takes them more time to get to the destination, resulting in raising the entire temperature. Thus, as the number of neighboring nodes is reduced, the total temperature of the network gets higher.

4.1.2. Packet generation rate versus hop count per arrived packet

Next, we simulate the relation between the packet generation rate and hop count per arrived packet in regarding three routing algorithms. This metric also can be translated into the average cost or delay for packets to get to the destination because as the number of hop counts increases, a packet is apparently delivered to the destination in a longer time.

From Figure 8, hop count per arrived packet does not seem to have any relation to the packet generation rate. Instead, all three algorithms experience relatively stable hop counts in the entire simulation.

However, the degree of the average hop count varies from one algorithm to another. LTRT is, in general, designed to choose a route in which the sum of the temperature of forwarding sensor nodes is the least. Therefore, LTRT is considered to have advantages of both SHR and LTR, that is, LTRT is considered as a hybrid of SHR and LTR. Since LTRT is concerned with both the shortest hop count and the least temperature, the average hop count is much lower than LTR and ALTR. On the other hand, LTR initially does not know the direction of the destination unless a sensor node having a packet neighbor as the destination, and only concerns about the temperature of the neighboring nodes but not about the temperature of the total network. Thus, LTR is apt to choose a neighboring node that has the least temperature even though it is located opposite to the destination. Therefore, while LTR raises the temperature of individual sensor nodes a little, regarding the temperature of the entire network, it raises the temperature higher and faster than LTRT.

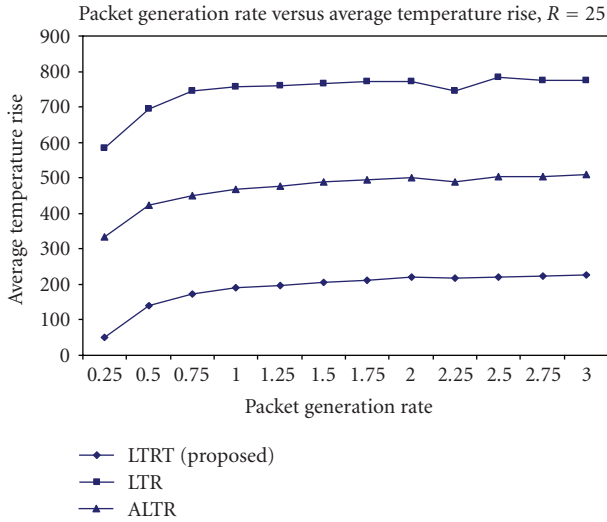


FIGURE 7: Packet generation rate versus average temperature rise with radio transmission range 25.

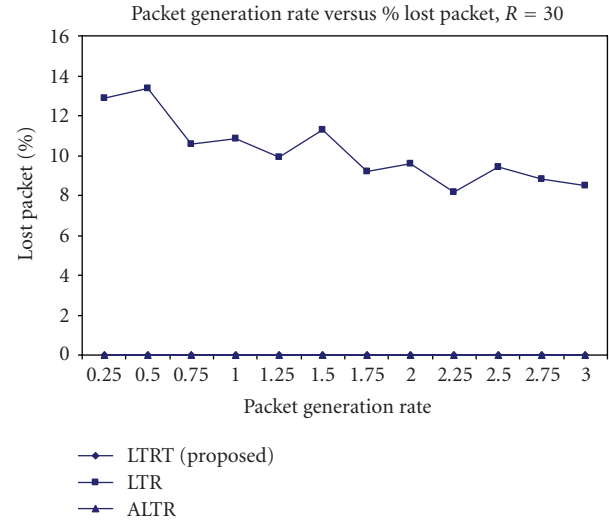


FIGURE 9: Packet generation rate versus percentage of lost packet.

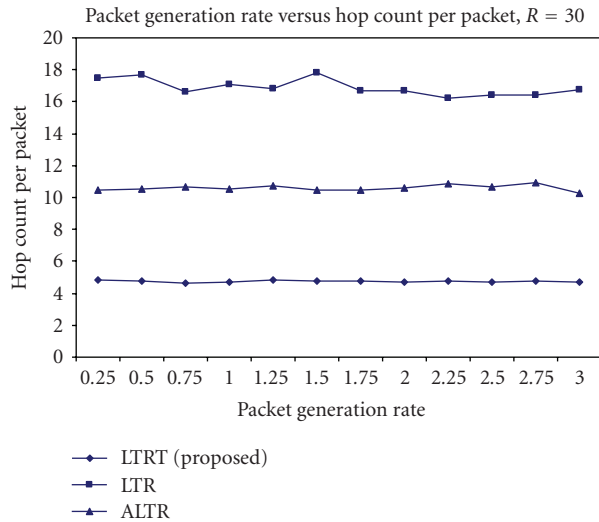


FIGURE 8: Packet generation rate versus hop count per arrived packet.

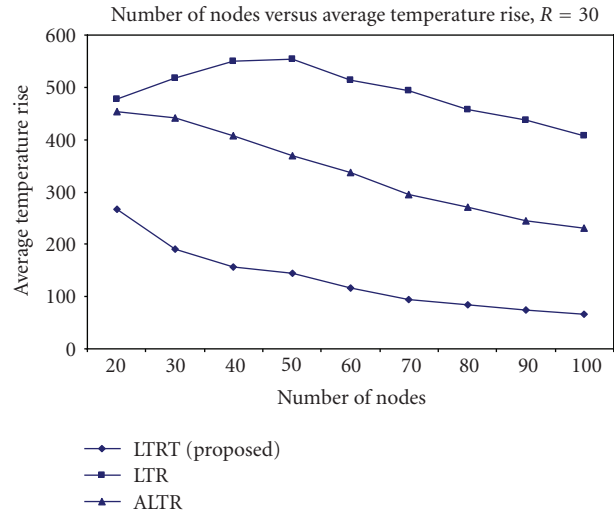


FIGURE 10: Number of sensor nodes versus average temperature rise.

4.1.3. Packet generation rate versus percentage of the lost packet

Regarding the total lost packets, shown in Figure 9, LTR has relatively high ratio based on the total number of sending packets, and this is easily explained by the result of the simulation of the packet generation rate versus hop counts per arrived packet. The previous simulation showed us that LTR takes packets more time to arrive at the destination, and this increases the probability that packets exceed a predefined maximum hop count threshold. Moreover, since LTRT and ALTR are designed to send almost every packet to the destination eventually, the percentage of the lost packets is very close to zero.

4.2. Scalability simulation

In this simulation, we investigate the tendency of the temperature rise, total hop counts per arrived packet, and percent-

age of the lost packet in terms of the number of sensor nodes in the network. The scalability is measured in the range of 20 to 100, and in each case, we simulate the temperature rise and other metrics by operating the three thermal-aware routing algorithms: LTR, ALTR, and LTRT.

4.2.1. Number of sensor nodes versus average temperature rise

As the number of sensor nodes increases, since all the three thermal-aware routing algorithms can disperse routings throughout the entire network, the average temperature basically decreases. Therefore, ALTR and our proposed LTRT represent this tendency well in Figure 10. In LTR, however, the average temperature gradually increases as the number of nodes increases up to 50 sensor nodes. This is because, the more the number of nodes becomes, the more chances the packets get to trace extra nodes whose temperature is

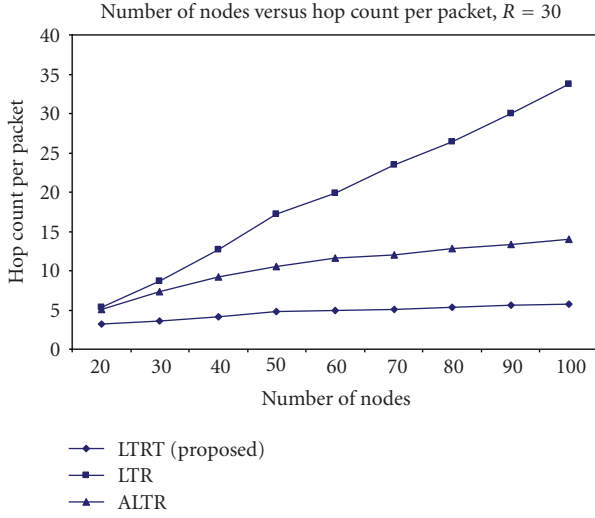


FIGURE 11: Number of sensor nodes versus hop counts per arrived packet.

comparatively low until arriving at the destination. In other words, as the number of sensor nodes increases, the number of choices of routes from the sender to the destination also increases. Therefore, the packets are attempted to roam more around the entire network, and this causes the temperature of the entire network to become higher. Moreover, as the number of nodes exceeds 50, the distance from the senders to the destinations also becomes longer, and because packets tend to exceed a predefined hop count threshold, they are dropped out of the network and cannot increase the route temperature anymore so that the average temperature gradually decreases.

4.2.2. Number of sensor nodes versus hop counts per arrived packet

Figure 11 shows the tendency of the hop count rise based on the number of sensor nodes. As we have already mentioned in the previous section, as the number of sensor nodes grows, choices of routes from the sender to the destination also increase. In general, this helps the temperature averaging over all the sensor nodes in the network decrease. In LTR, however, since packets always choose the least temperature nodes until they arrive at the destination or exceed a predefined threshold, directions are not necessarily toward the destination. Thus, in LTR and ALTR, packets are attempted to select these low-temperature nodes instead of directly going toward the destination nodes. In case of a network with 100 sensor nodes, the number of hop counts per arrived packet of LTR almost reaches 40. Therefore, in 100 sensor nodes, almost all packets are discarded from the network. One solution to avoid this situation is to let the packets have more hop counts. However, since this solution also allows packets to roam around the network longer, the temperature of the entire network will also increase.

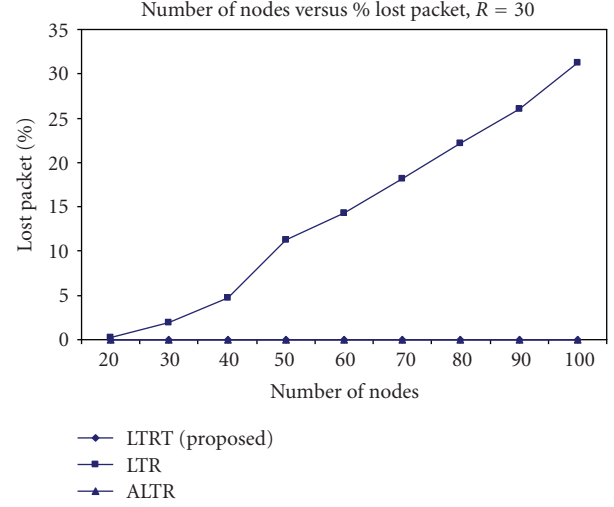


FIGURE 12: Number of sensor nodes versus percentage of lost packet in case of radio transmission range 30.

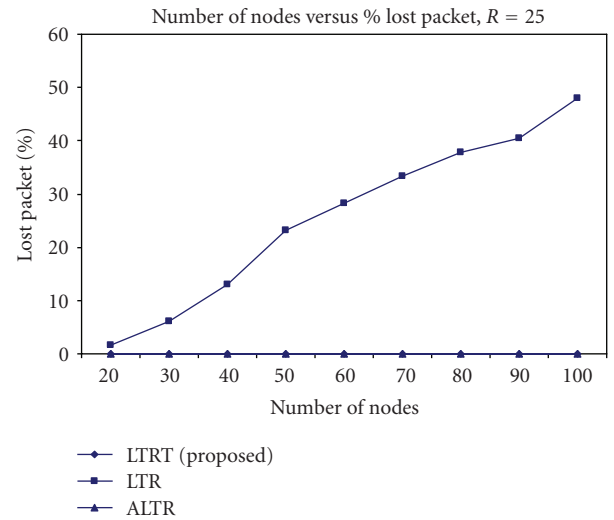


FIGURE 13: Number of sensor nodes versus percentage of lost packet in case of radio transmission range 25.

4.2.3. Number of sensor nodes versus percentage of lost packet

We investigate the relation between the number of sensor nodes and lost packets out of 2000 generated packets. The results are shown in Figures 12 and 13. In Figure 12, this is the case that radio transmission range of each sensor node is equal to 30 so that every node can have neighbors in the range from 3 up to 8. Moreover, in Figure 13, their radio transmission range is restricted up to 25 so that sensor nodes have no more than 4 or less neighbors.

Both figures show the same tendency similar to that in LTR, as the number of sensor nodes increases in the network, the percentage of lost packet grows, and these results

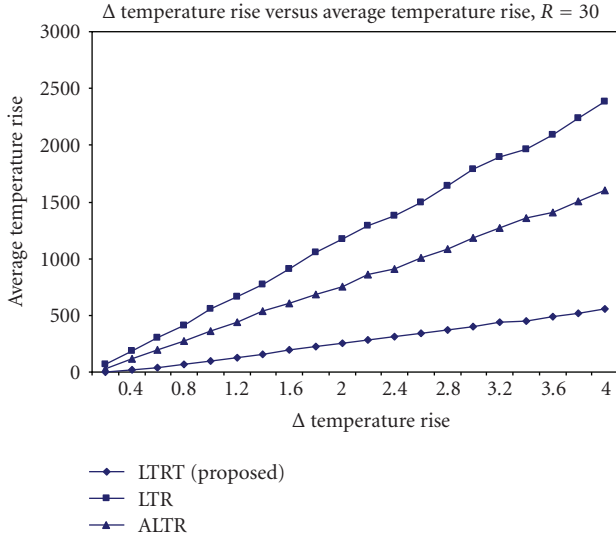


FIGURE 14: Δ temperature rise versus average temperature rise.

are explained in the previous simulation, that is, the number of sensor nodes versus hop counts per arrived packet. In the previous simulation, as the number of sensor nodes increases, the number of hop counts per arrived packet also increases in LTR. Since as the number of hop counts increases, the probability that packets exceed a predefined threshold also gets higher, and this probability directly affects the percentage of lost packet.

Meanwhile, both ALTR and our proposed LTRT show much efficiency about the lost packets that is close to zero. In ALTR, routing algorithm can be changed from LTR to SHR, whose objective is to send packets to the destination as soon as possible, after packets exceed a predefined threshold. LTR experiences much more lost packets than the other two algorithms, where almost half of the sending packets are discarded in case of radio transmission range 25. This tendency just shows that the network is unreliable.

4.3. Δ temperature rise versus average temperature rise

We investigate the relation between settings of Δ temperature rise and the average temperature rise in Figure 14. In short, Δ temperature rise means how much temperature of each node increases when it receives a packet from the neighboring nodes. In previous simulations, we just set this value to one temperature unit, which is constant. However, we figure out that as we gradually increased Δ temperature, since the total network temperature is calculated by the product of Δ temperature rise and the total hop counts performed in the network, the average temperature of the networks in LTR and ALTR goes up faster than LTRT. Thus, from the application perspective, reducing the total hop counts of each packet is one solution to suppress the total or average temperature rise of the network. In other words, how to control the total hop count by routing algorithms is very important.

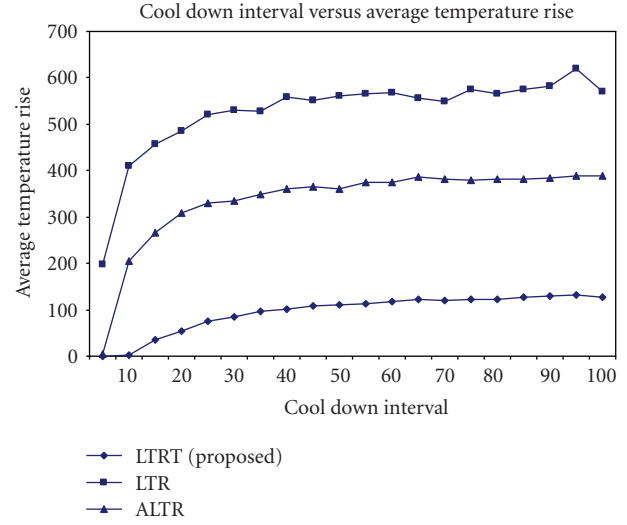


FIGURE 15: Cool-down interval versus average temperature rise.

4.4. Cool-down interval versus average temperature rise

Figure 15 shows the relation between the cool-down intervals and average temperature rises. It shows how the average temperature rise will change when the cool-down interval gets longer. Basically, each implementation of the simulation takes around 2000 units of time. Thus, in case of setting the cool-down interval with 5 units of time, the cool-downs are conducted 400 times in each simulation, and this can be translated that total 400 units of temperature are reduced from the total temperature or 8 units of temperature are reduced from each node. On the other hand, when we set the cool-down interval with 100 units of time, the simulation experienced only 20 cool-down events, and this means that totally no more than 20 units could be reduced from the total temperature.

In general, every thermal-aware routing algorithm shows ascent of its trend as the cool-down interval gets longer. However, in Figure 15, in the first ascending trend, LTRT shows relatively gentle temperature rise, while in LTR and ALTR, the average temperatures witness a rapid increase by more than 200 units. Therefore, although after these steep rises of the average temperature both of the ascending trends gradually slow down, both of LTR and ALTR record higher average temperatures than that of LTRT.

This simulation shows us that the cool-down interval is also an important parameter affecting the average temperature of every sensor node. However, since this parameter largely relies on inside temperature of the human bodies, generally by no means, can this parameter be controlled by the application of the biomedical sensors themselves.

4.5. Level of hot spot versus number of packets passing hot spots

In Figure 16, we gradually change the point of the hot spot, where the packet generation rate is 1 and the number of sen-

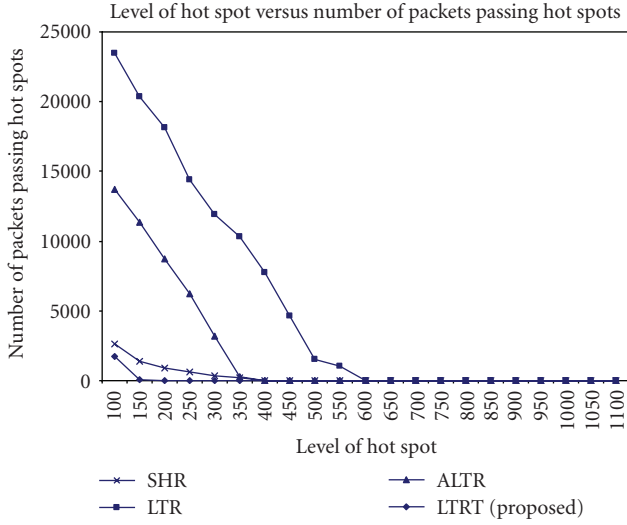


FIGURE 16: Level of hot spot versus number of packets passing hot spots.

sensor nodes is 50. The simulation starts with hot spot point 100, which means that sensor nodes that have more than 100 units of temperature are considered as hot spots. This hot spot point is thought to be low because even LTRT experiences about 100 units of the average temperature rise. Figure 16 shows that for every routing algorithm, packets experience more or less hot spot passing. However, as we mentioned that LTRT generates only about 100 units of the average temperature, after we set the point of the hot spot with 100, almost no packet experiences hot spot passing. Moreover, since LTR and ALTR generate relatively high average temperatures, even though the number of packets passing hot spots decreases, packets are still required to choose hot spots on their routing paths even after the hot spot is set with 300. The previous simulations show that LTR generates the average temperature rise near 600 units of temperature, and packets keep experiencing hot spot passing up to hot spot set with 600.

For LTR and ALTR, when they generate the average temperature more than the level of the hot spot, almost all sensor nodes have temperature over the hot spot. However, this situation is critical in thermal-aware routing applications.

Our assumption is that fewer hop counts generate fewer hot spots and consequently less average temperature. Therefore, even the shortest hop routing (SHR) algorithm generates better performance than LTR and ALTR in terms of the hot spot. However, since SHR concerns about the hop count rather than temperature, even though it generates comparatively low average temperature rise, which is close to those generated by LTRT, it still experiences the hot spot passing at higher hot spot settings than that of LTRT.

4.6. Packet generation rate (PGR) versus percent of hot spot passed by packets

Figure 17 presents the transition of how many hot spots packets pass by as the packet generation rate increases. In this simulation, a hot spot is set up with 300 units of temperature,

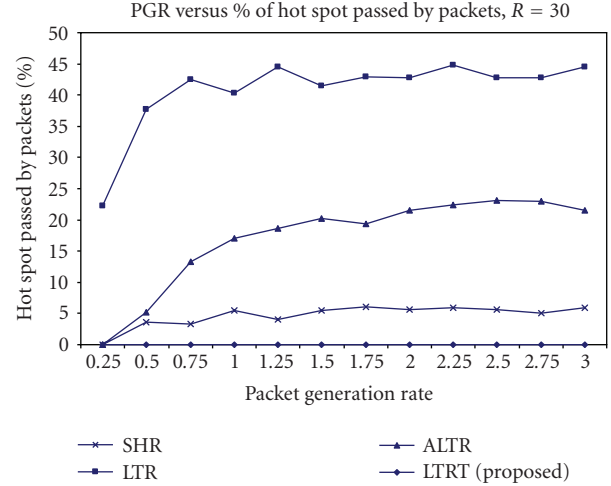


FIGURE 17: Packet generation rate versus number of hot spots passed by packets with radio transmission range 30.

and the ratio of the number of hot spots passed by packets to the total hops is calculated. As we have mentioned in the previous simulations, since the average temperature rise gets higher as the packet generation rate increases, the probability that packets choose routing paths which partially contain hot spots also gets higher. Figure 17 just shows this tendency.

In LTRT, the average temperature rise is comparatively low, which is no more than 150, and because of its nature of avoidance of hot spots, no packet goes through hot spots in the execution. On the other hand, although SHR generates almost the same average temperature rise as those in LTRT, packets still need to pass through hot spots in every execution except for packet generation rate of 0.25, where they record about 5% of the total hop count.

However, in LTR and ALTR, things get worse than SHR, and about 45% and 20% of the total hops pass over the hot spots, respectively. Since both of the algorithms experience the higher average temperature rise, packets basically experience more hot spot passing even though they are attempted to avoid passing hot spots by always choosing the least temperature nodes. One weakness of these algorithms is that because the packets select the least temperature neighbor nodes as their routing paths every time, the temperature of every node evenly gets higher as the process goes on. Therefore, when the average temperature exceeds a hot spot setting, almost every node has temperature exceeding the hot spot temperature. Consequently, the later probability that packets will pass through hot spots becomes much higher than those of LTRT and SHR.

4.7. Number of nodes versus percent of hot spot passed by packets

As described in the previous simulations, the number of nodes and the average temperature rise are, in general, inversely related. Therefore, as the number of nodes increases, the ratio of the number of hot spots passed by packets to the

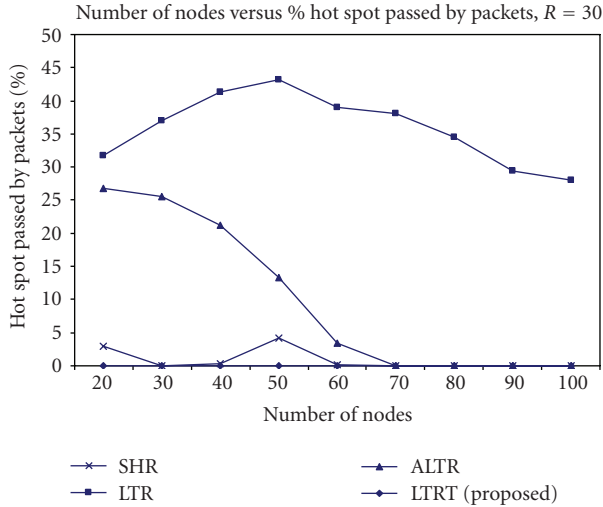


FIGURE 18: Packet generation rate versus percentage of hot spot passed by packets with radio transmission range 30.

total hop count decreases. However, since LTR generates over 400 units of temperature rise even with 100 nodes, 1/3 of hops are still required to pass over hot spots in LTR with 100 sensor nodes. On the other hand, after the number of nodes exceeds 60, ALTR keeps its average temperature below 300. Since then, no packet experiences hot spot passing.

Furthermore, although, as the number of nodes increases, the probability that packets pass through the hot spots gets lower, in SHR, the packets still have chances to select the hot spots as part of their routing paths. In the figure above, occasionally SHR generates about 5% of the hot spot passing even though in other cases, it becomes lower or none.

5. CONCLUSIONS

This paper proposed a thermal-aware routing algorithm called the least total-routing-temperature (LTRT) algorithm that mainly concerns about both the shortest hop count and the least temperature rise of the entire network. It is a hybrid of the shortest hop-count routing (SHR) algorithm and the least temperature routing (LTR) algorithm described in [1]. Our thermal-aware routing algorithm is based on the single source shortest path (SSSP) in the graph theory and is modified such that the temperature of sensor nodes is transferred to the weight of outgoing edges so that the SSSP can choose a route where the sum of temperatures of forwarding nodes is the least. Since LTRT aims to send packets with nearly the shortest hop counts, it prevents the entire network temperature from rising quickly. Also, since LTRT concerns about the total temperature of selected routes, instead of choosing the shortest hop count routes having comparatively high temperature, it is attempted to detour sensor nodes that have high temperature and cause the route temperature to be high.

To evaluate the efficiency of our proposed algorithm, we performed extensive simulations comparing LTRT with LTR and the adaptive least temperature routing (ALTR) algorithm [1] in terms of temperature rising or other efficiencies. Our simulation results show that packets experience low hop

counts up to the destination compared with LTR and ALTR. On the other hand, in LTR and ALTR, prior to a predefined threshold, sender nodes always choose the least-temperature neighbor node for their route so that packets can keep roaming in the network in a longer period of time than SHR and LTRT. Thus, in the simulations, both LTR and ALTR always recorded higher temperature than the proposed LTRT. In addition, we also performed a couple of simulations in terms of the scalability of all the three thermal-aware algorithms. In these simulations, LTRT shows good performance in terms of temperature rise, hop counts per arrival packet, and percentage of lost packets. LTR largely degrades its performance, especially about the number of hop counts and lost packets. In particular, in case of 100 sensor nodes, in LTR, almost half of the generated packets are discarded due to an excess of hop counts, and this, to a great extent, degrades the reliability of the sensor network.

In our future research, we will keep exploring more details about the thermal-aware routing algorithms and also design more optimal solutions or alternatives. Moreover, we will design the architecture and real application with scenarios adopting our proposed routing algorithm. The proposed scheme can be used in remote cardiac patients monitoring applications in [14, 15].

ACKNOWLEDGMENTS

This work is partially supported by the US National Science Foundation (NSF) under Grants no. CNS-0716211 and CNS-0716455. The work of Zhejiang University is partially supported by the National Natural Science Foundation of China (NSFC) under Grant no. 60604029, and by Joint Funds of NSFC-Guangdong under Grant no. U0735003.

REFERENCES

- [1] A. Bag and M. A. Bassiouni, "Energy efficient thermal aware routing algorithms for embedded biomedical sensor networks," in *Proceedings of the 1st IEEE International Workshop on Intelligent Systems Techniques for Wireless Sensor Network in conjunction with the 3rd IEEE International Conference on Mobile Ad-hoc and Sensor Systems*, pp. 604–609, Vancouver, BC, Canada, October 2006.
- [2] L. Schwiebert, S. K. S. Gupta, and J. Weinmann, "Research challenges in wireless networks of biomedical sensors," in *Proceedings of the 7th Annual International Conference on Mobile Computing and Networking (MobiCom '01)*, pp. 151–165, Rome, Italy, July 2001.
- [3] L. Schwiebert, S. K. S. Gupta, P. S. G. Auner, G. Abrams, R. Iezzi, and P. McAllister, "A biomedical smart sensor for the visually impaired," in *Proceedings of the IEEE Sensors*, vol. 1, pp. 693–698, Orlando, Fla, USA, June 2002.
- [4] C. Furse, H. K. Lai, C. Estes, A. Mahadik, and A. Duncan, "An implantable antenna for communication with implantable medical devices," in *Proceedings of the IEEE Antennas and Propagation/ URSI International Symposium*, Orlando, Fla, USA, July 1999.
- [5] C. Furse, R. Mohan, A. Jakayar, et al., "A biocompatible antenna for communication with implantable medical devices," in *Proceedings of the IEEE International Symposium on Antennas and Propagation*, San Antonio, Tex, USA, June 2002.

- [6] Q. Tang, N. Tummala, S. K. S. Gupta, and L. Schwiebert, "TARA: thermal-aware routing algorithm for implanted sensor networks," in *Proceedings of the 1st IEEE International Conference on Distributed Computing in Sensor Systems (DCOSS '05)*, vol. 3560 of *Lecture Notes in Computer Science*, pp. 206–217, Marina del Rey, Calif, USA, June-July 2005.
- [7] Y. Prakash, S. Lalwani, S. K. S. Gupta, E. Elsharawy, and L. Schwiebert, "Towards a propagation model for wireless biomedical applications," in *Proceedings of the IEEE International Conference on Communications (ICC '03)*, vol. 3, pp. 1993–1997, Anchorage, Alaska, USA, May 2003.
- [8] W. R. Heinzelman, A. Chandrakasan, and H. Balakrishnan, "Energy-efficient communication protocol for wireless microsensor networks," in *Proceedings of the 33rd Hawaii International Conference on System Sciences (HICSS '00)*, vol. 8, p. 8020, Maui, Hawaii, USA, January 2000.
- [9] V. Shankar, A. Natarajan, S. K. S. Gupta, and L. Schwiebert, "Energy-efficient protocols for wireless communication in biosensor networks," in *Proceedings of the 12th IEEE International Symposium on Personal, Indoor and Mobile Radio Communications (PIMRC '01)*, vol. 1, pp. D114–D118, San Diego, Calif, USA, September 2001.
- [10] Y. Xiao, X. Shen, B. Sun, and L. Cai, "Security and privacy in RFID and applications in telemedicine," *IEEE Communications Magazine*, vol. 44, no. 4, pp. 64–72, 2006.
- [11] F. Hu, S. Kumar, and Y. Xiao, "Towards a secure, RFID/sensor based tele-cardiology system," in *Proceedings of the 4th IEEE Consumer Communications and Networking Conference (CCNC '07)*, pp. 732–736, Las Vegas, Nev, USA, January 2007.
- [12] Y. Xiao and F. Hu, "Wireless telemedicine and M-health," in *Proceedings of the 4th IEEE Consumer Communications and Networking Conference (CCNC '07)*, pp. 727–731, Las Vegas, Nev, USA, January 2007.
- [13] Y. Xiao, D. Takahashi, and F. Hu, "Telemedicine usage and potentials," in *Proceedings of the IEEE Wireless Communications and Networks Conference (WCNC '07)*, pp. 2736–2740, Kowloon, China, March 2007.
- [14] F. Hu, M. Jiang, and Y. Xiao, "Low-cost wireless sensor networks for remote cardiac patients monitoring applications," 2007, to appear in *Wireless Communications and Mobile Computing Journal*.
- [15] F. Hu, M. Jiang, L. Celentano, and Y. Xiao, "Robust medical ad hoc sensor networks (MASN) with wavelet-based ECG data mining," 2007, to appear in *Ad Hoc Networks*.
- [16] Y. Xiao and H. Chen, Eds., *Mobile Telemedicine: A Computing and Networking Perspective*, Auerbach Publications, Taylor & Francis, New York, NY, USA, 2007.
- [17] Q. Alexander, Y. Xiao, and F. Hu, "Telemedicine for pervasive healthcare," in *Mobile Telemedicine: A Computing and Networking Perspective*, Auerbach Publications, Taylor & Francis, New York, NY, USA, 2008.
- [18] L. Biggers, Y. Xiao, and F. Hu, "Conventional telemedicine, wireless telemedicine, sensor networks, and case studies," in *Mobile Telemedicine: A Computing and Networking Perspective*, Auerbach Publications, Taylor & Francis, New York, NY, USA, 2008.
- [19] F. Hu, M. Lewis, and Y. Xiao, "Automated blood glucose management techniques through micro-sensors," in *Mobile Telemedicine: A Computing and Networking Perspective*, Auerbach Publications, Taylor & Francis, New York, NY, USA, 2008.
- [20] D. Takahashi, Y. Xiao, and F. Hu, "A survey of security in telemedicine with wireless sensor networks," in *Mobile Telemedicine: A Computing and Networking Perspective*, Auerbach Publications, Taylor & Francis, New York, NY, USA, 2008.
- [21] F. Hu, L. Celentano, and Y. Xiao, "Mobile secure telecardiology based on wireless and sensor networks," in *Mobile Telemedicine: A Computing and Networking Perspective*, Auerbach Publications, Taylor & Francis, New York, NY, USA, 2008.
- [22] D. Takahashi, Y. Xiao, F. Hu, and M. Lewis, "A survey of insulin-dependent diabetes part I: therapies and devices," to appear in *International Journal of Telemedicine and Applications*.
- [23] J. Chen, K. Cao, Y. Sun, Y. Xiao, and X. Su, "Continuous drug infusion for diabetes therapy: a closed-loop control system design," to appear in *EURASIP Journal on Wireless Communications and Networking*.